Sub-Part-per-Billion Analysis of Aqueous Lead Colloids by ArF Laser Induced Atomic Fluorescence

ARTICLE *in* ANALYTICAL CHEMISTRY · FEBRUARY 2005

Impact Factor: 5.64 · DOI: 10.1021/ac048764a · Source: PubMed

2 AUTHORS:

Sut Kam Ho
University of Macau
19 PUBLICATIONS **97** CITATIONS
SEE PROFILE

Nh Cheung
Hong Kong Baptist University
53 PUBLICATIONS **937** CITATIONS
SEE PROFILE

Anal. Chem. **2005,** *77,* 193−199

Sub-Part-per-Billion Analysis of Aqueous Lead Colloids by ArF Laser Induced Atomic Fluorescence

S. K. Ho[†,‡] and N. H. Cheung*[,†]

Department of Physics, Hong Kong Baptist University, Kowloon Tong, Hong Kong, China, and Faculty of Science and Technology, University of Macau, Macau, China

Highly sensitive analysis of aqueous lead carbonate colloids was demonstrated by two-pulse laser-induced atomic fluorescence. The first laser pulse at 1064 nm ablated the sample solution to create an expanding plume. The colloids, being heavier, trailed behind and became concentrated. They were then intercepted by an ArF laser pulse that induced prompt atomic fluorescence at 405.8 nm from the lead atoms. The detection limit for lead was 0.24 ppb. Tap water was analyzed, and lead emissions were clearly observed. Time-resolved spectroscopy revealed that the efficient 193-nm excitation of the analytes was more universal than expected. That was confirmed by the successful application of the technique to colloids and alloys other than lead.

The grave toxicity of lead was not well understood until the 1980s, partly because of the inadequate sensitivity of earlier analytical methods.[1] It is now known that lead pollutants can assume all three states: gaseous as in incinerator and smelter fumes and automobile exhaust; aqueous in the form of dissolved lead ions; and solids as found in dried paints, solders, pipes, soil, and minerals. Contrary to common belief, insoluble compounds of lead, when present as submicrometer particulates, are taken up as efficiently as soluble forms either through the pulmonary tract when inhaled or through the gastrointestinal tract if ingested.[2] It was also suggested that lead in drinking water might be promptly absorbed because the stomach could well be in semifasting conditions between meals.

Trace amounts of lead in water, especially colloidal forms, can be extremely common. Gaseous lead pollutants are known to react in the atmosphere to form insoluble oxides and sulfates. They deposit in soil to be eventually transported by groundwater. Chips from paints, usually in the form of lead carbonates and oxides, can be dispersed as dust or aerosols and again find their way to reservoirs and streams. Yet the most alarming is the high level of lead, both dissolved and colloidal, in household tap water.[3] The high levels are not because of inadequate treatment at water plants, but rather because of distribution plumbing and faucets. The situation worsens with the standing time of water in such lines, as evidenced by the high lead contents in first drawn water in the morning or after weekends and long vacations at schools and offices.

In the United States, the allowed level of lead in drinking water is presently set at 15 part-per-billion (ppb) by weight, to be revised down to "zero" when both purification and detection technology permits.[4] To detect lead at the ppb level, the only viable technology is inductively coupled plasma mass spectrometry (ICPMS). When applied to the analysis of lead colloids, the sample preparation and digestion step can be time-consuming and involved.

A simpler and more versatile technique is the all-optical laser-induced plasma spectroscopy (LIPS) when specimens are analyzed real time and on-line without the need for sample preparation. It has been successfully applied to the analysis of particulates. Notable examples include aerosol analysis for air quality assurance[5] and particle counting in water purification plants.[6] We recently demonstrated a two-pulse LIPS analysis of aqueous lead colloids.[7] The first pulse created a vapor plume with the particulates concentrated in space because of slower propagation. They were then ablated by an ArF laser pulse that efficiently atomized and excited the lead analytes. Lead emissions at 405.8 nm were detected. A detection limit of 14 ppb was achieved, which was 3 orders of magnitude more sensitive than conventional LIPS analysis of lead ions in water.[8] Nonetheless, our sensitivity was only marginally adequate for the present task.

An interesting modification of our previous setup was to use the 193-nm laser to induce atomic lead fluorescence instead of plasma emissions. The spectral background could be significantly reduced for enhanced detection sensitivity. Extensive work has

* Corresponding author. E-mail: nhcheung@hkbu.edu.hk.
† Hong Kong Baptist University.
‡ University of Macau.

(1) For a comprehensive review of lead toxicity and environmental pollution, see: The National Academy of Sciences. *Measuring lead exposure in infants, children, and other sensitive populations*; National Academy Press: Washington, DC, 1993. This is downloadable from www.nap.edu/openbook/030904927X/R15.html.

(2) Rabinowitz, M. B.; Kopple, J. D.; Wetherill, G. W. *Am. J. Clin. Nutr.* **1980**, *33*, 1784−1788.

(3) According to a study done by the U.S. Environmental Protection Agency in 1987, more than 50% of household tap water has lead above the allowed level (20 ppb then) in the first few flush. See ref 1.

(4) See, for example, the Lead Toxicity page of the website of the U.S. Agency for Toxic Substances and Disease Registry: www.atsdr.cdc.gov?HEC/CSEM/lead.

(5) Carranza, J. E.; Hahn, D. W. *Anal. Chem.* **2002**, *74*, 5450−5454.

(6) Bundschuh, T.; Knopp, R.; Winzenbacher, R.; Kim, J. I.; Koster, R. *Acta Hydrochim. Hydrobiol.* **2001**, *29*, 7−15.

(7) Pu, X. Y.; Ma, W. Y.; Cheung, N. H. *Appl. Phys. Lett.* **2003**, *83*, 3416−3418.

(8) Knopp, R.; Scherbaum, F. J.; Kim, J. I. *Fresenius J. Anal. Chem.* **1996**, *355*, 16−20.

10.1021/ac048764a CCC: $30.25
Published on Web 12/01/2004

been done on excimer laser fragmentation fluorescence when gaseous precursor molecules were photodissociated to produce excited analyte atoms.[9] More recently, dried aerosols of lead salts were analyzed by fragmenting at 193 nm and monitoring at 405.8 nm.[10] It should be useful to combine the two-pulse and fluorescence techniques to analyze aqueous lead colloids: The first laser pulse to concentrate the precursor analytes and the second pulse at 193 nm to induce atomic lead fluorescence for ultrasensitive detection.

In what follows, we will report our investigation of two-pulse ArF laser-induced atomic lead fluorescence off colloidal lead. We will show that the excitation mechanism is interesting and sub-ppb detection sensitivity is possible. We will report our analysis of household tap water as well as other colloidal systems and bulk alloy targets to establish the practicality and universality of the technique.

EXPERIMENTAL SECTION

Sample Preparation. Lead carbonate colloids were chosen as the test sample because of their stability and prevalence. The colloids were prepared by mixing solutions of $Pb(NO_3)_2$ and Li_2CO_3. It was found that the concentrations of reagents and the order of mixing (Pb^{2+} into CO_3^{2-} or vice versa) would affect the size of the product colloids. To produce particulates of ~200 nm in diameter, the samples were prepared by adding x volume of 5.91 mM $Pb(NO_3)_2$ to 400 mL of 0.155 mM Li_2CO_3, where x determined [Pb] in the sample. Once prepared, the samples were used within 1 day, when the colloids were found to be stable against aggregation or dissolution.

Colloids of lead oxide and iron oxide were produced by mixing granular oxide powders with surfactants (sodium dodecyl sulfate), ground in a ball grinder, and then suspended in water. Gold colloids of 100- and 250 -nm diameter were used as bought.

Target surfaces of bulk lead and alloys of copper and aluminum were first laser-cleaned before analysis.

Signal Detection. The present scheme evolved from our earlier LIPS approach.[7] The setup, shown schematically in Figure 1, was similar to the one reported and so the description here will be brief. The colloid solution was ejected from a flow cell through a 0.5-mm-i.d. glass tubing in the form of a stable vertical stream. The sample jet flowed along $-z$ into the plane of the paper (Figure 1) and was ablated downstream by a Nd:YAG laser pulse (1064 nm, 6 ns, 10 Hz, 60 mJ/pulse) focused to ~0.5-mm diameter. The 1064-nm beam was horizontal, 30° from the collection optics axis, and directed at the center of the jet. The induced vapor plume expanded along a direction nearly antiparallel to the 1064-nm laser beam. After 2.5 μs, the plume was intercepted by an ArF laser pulse (193 nm, 10 ns, 10 Hz, 60 mJ/pulse) focused to 3 mm × 0.5 mm. The ArF laser fluence was therefore only 4 J cm^{-2} instead of the 13 J cm^{-2} used in our previous LIPS analysis.

The luminous plume was imaged (1:2, magnified) onto the entrance slit of a 0.5-m spectrograph equipped with a 2400 lines/mm grating. The slit width was set to 220 μm, giving an overall spectral resolution of ~0.2 nm. Except for the intensely bright core, the rest of the luminous plume was imaged onto the relatively wide slit. Emission signals were detected by a gateable intensified charge-coupled device (ICCD) mounted at the exit plane of the spectrograph. It was gated on 30 ns before the firing of the ArF laser and remained on for 100 ns. Such gate settings maximized the ratio of the Pb signal to the background noise. The emission spectrum was obtained by accumulating 300 events. All the spectra displayed were smoothed with a 9-pixel sliding average, which was equivalent to a 0.07-nm window. The instrumental resolution of 0.2 nm was well preserved.

As can be seen, except for the lower laser fluences, the setup was identical to conventional LIPS experiments. This allowed switching between the two detection modes for complementary information.

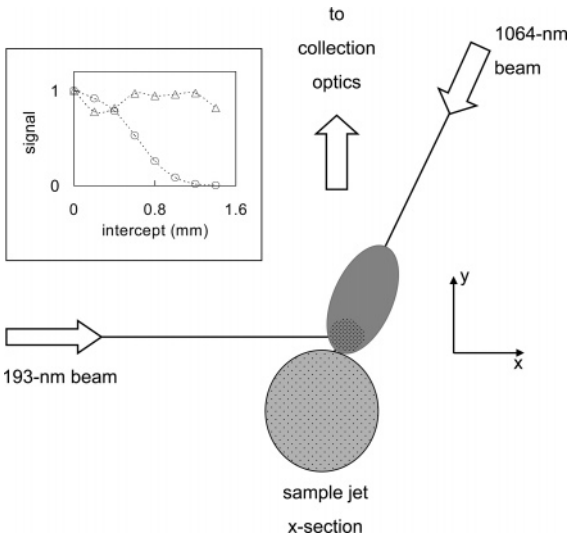

Figure 1. Schematics of the two-pulse ArF-LEAF setup, as viewed from the top. Inset shows the Pb 405.8-nm signal as the ArF beam was scanned along *y*. The maximum signal was normalized to one. When a colloid solution was sampled (open circles), more Pb was detected near the plume base. When a solution of dissolved lead nitrate was sampled (open triangles), Pb was extensively dispersed.

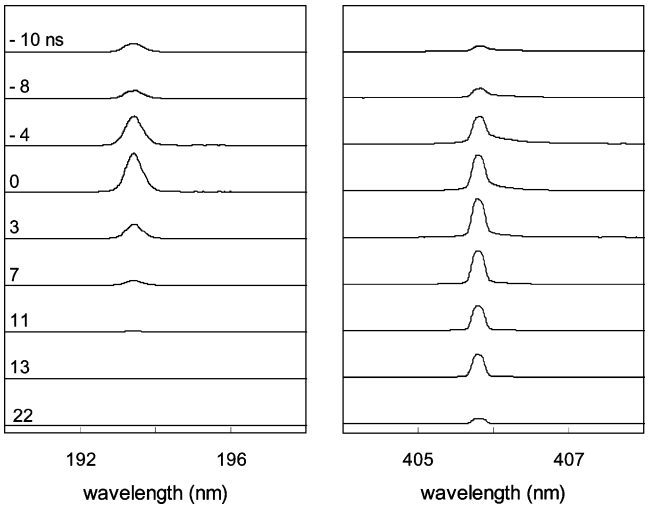

Figure 2. Time-resolved spectra of the ArF laser pulse at 193 nm (left panel) and the 405.8-nm Pb I emissions induced by it off lead carbonate colloids (right panel). The lead concentration was 1 ppm. The gate width of the ICCD was 11 ns, giving an optical width of ~2.5 ns. The peak of the ArF pulse was defined as time zero.

(9) Simeonsson, J. B.; Sausa, R. C. *Appl. Spectrosc. Rev.* **1996**, *31*, 1−72.
(10) Buckley, S. G.; Sawyer, R. F.; Koshland, C. P.; Lucas, D. *Combust. Flame* **2002**, *128*, 435−446.

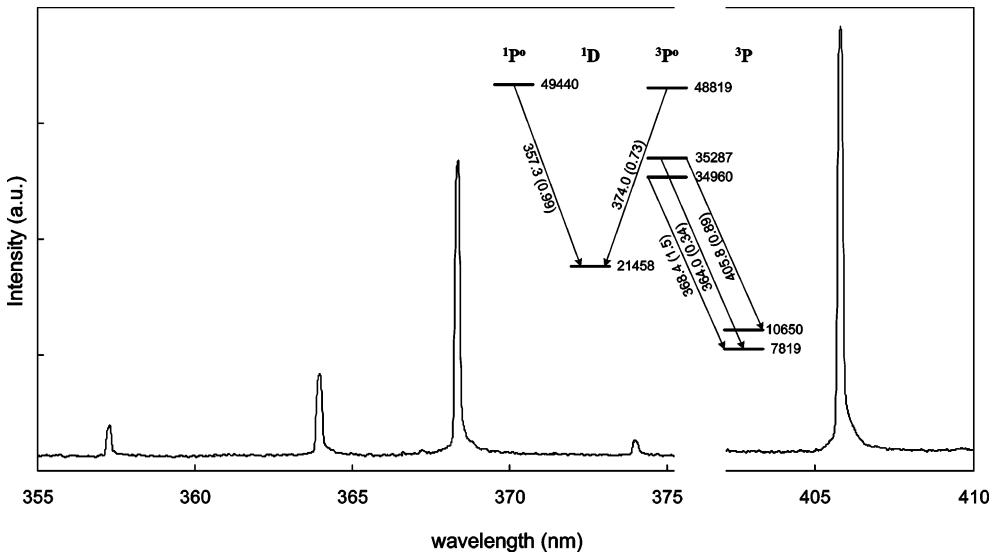

Figure 3. A panoramic scan of the prompt emissions of all the Pb I lines generated by two-pulse ArF-LEAF analysis of lead carbonate colloids suspended in water. The [Pb] was 500 ppb. Four spectra taken separately were stitched. The relevant Grotrian diagram was also shown, with the level energy in cm^{-1}, transition wavelength in nm, and Einstein *A* coefficient in 10^8 s^{-1}.

RESULTS AND DISCUSSION

We will report our experimental results in terms of (1) signal lifetime, (2) excitation mechanism, and (3) analytical performance. Contrasts against our earlier LIPS findings will be highlighted.[7]

ArF Laser-Induced Prompt Signal. In our earlier LIPS analysis of aqueous $PbCO_3$ colloids, lead emissions at 405.8 nm were observed once the continuum background had decayed sufficiently.[7] The signal lasted for several microseconds, as expected of LIPS emissions. In the present experiment, however, the 405.8-nm emissions were synchronous with the ArF laser pulse and lasted for only tens of nanoseconds. This is shown in Figure 2. Because of the lower ArF laser fluence, the plasma continuum background was significantly reduced and prompt 405.8-nm emissions were easily observed. Similar prompt emissions were observed by another group when PbO aerosols were irradiated at 193 nm.[10] In that work, the emissions were attributed to ArF laser photofragmentation of PbO to produce excited Pb* that subsequently fluoresced.

Much like our previous LIPS analysis, the present prompt signal could be further enhanced if two laser pulses were used. The first laser pulse at 1064 nm and 30 J cm^{-2} ablated the colloids selectively without breaking down pure water excessively. The plume then expanded in space. The colloid particles, being heavier, trailed behind the vapor molecules and became concentrated. They were then ablated by a second laser pulse at 193 nm. The analyte signal at 405.8 nm was enhanced 15-fold relative to the single pulse case. This preconcentration effect was measured by translating a tighter focused 193-nm beam along the *y* direction (see Figure 1) to probe for Pb. The accumulation of lead near the plume base was evident from the inset in Figure 1 (open circles). If it were dissolved lead ion as opposed to colloids, lead vapor would disperse extensively in the expanding plume instead of being preconcentrated. This was also shown in the inset of Figure 1 (open triangles) when another aqueous specimen of dissolved lead ion was sampled.

In addition to the 405.8-nm emissions, equally prompt lead emissions at other wavelengths were observed. Their spectra, separately taken, were stitched and shown in Figure 3, together with the relevant Grotrian diagram. As can be seen, transitions from levels as high up as 6.13 eV (357.3 nm) were observed. Noting that each 193-nm photon was only 6.4 eV, single photon fragmentation fluorescence of PbX (X = O, Pb) could not account for the lead emissions observed.[11] We also scanned for PbO molecular spectral emissions,[12] and none were observed.

Two-photon 193-nm excitation was another possibility.[13] We looked for transitions from levels above 6.4 eV, and the 265.71-nm line was the only one tabulated.[14] Although it was not detected, the *A* coefficient for this transition was merely 10^4 s^{-1} so two-photon excitation could not as yet be ruled out.

Interestingly, the same prompt lead emissions were seen when bulk lead samples were ablated at 193 nm. Figure 4 shows the intensities of the 405.8 (circles)- and 357.3 (triangles)-nm lines as functions of ArF laser fluence. The emergence of signal at low but finite threshold fluence indicated that atomization and emissions were not one-step photoprocesses. Rather, atomization was probably caused by thermal vaporization,[15] and these lead atoms were induced to fluoresce by VUV photons. The very low threshold fluence also argued against two-photon processes.[16]

In brief, prompt (tens of nanoseconds) Pb I emissions were observed when lead carbonate colloids or bulk lead were ablated with ArF laser pulses at fluences below 5 J cm^{-2}. Transitions from atomic states as high up as 6.13 eV were seen. Lead atomization might be caused by thermal vaporization; to be followed by 193-nm laser excited atomic fluorescence (LEAF). Nevertheless, the

(11) Dissociation energies of PbO and Pb_2 are 3.8 and 0.9 eV, respectively. See: Radzig, A. A.; Smirnov, B. M., *Reference Data on Atoms, Molecules, and Ions*; Springer-Verlag: Berlin, 1985.

(12) Systems A−C of PbO from 360 to 670 nm. See: Pearce, R. W. B.; Gaydon, A. G. *The Identification of Molecular Spectra*, 4th ed.; Chapman & Hall: London, 1976; p 283.

(13) Gottwald, U.; Monkhouse, P. *Appl. Spectrosc.* **2003**, *57*, 117−123.

(14) Pb transitions of 265.71 nm. Moore, C. E. *Atomic Energy Levels as derived from analyses of optical spectra*; National Standards Reference Data Series; U.S. Government Printing Office: Washington, DC, 1971; Vol. 3, p 210.

(15) Arlinghaus, H. F.; Calaway, W. F.; Young, C. E.; Pellin, M. J.; Gruen, D. M.; Chase, L. L. *J. Appl. Phys.* **1989**, *65*, 281−289.

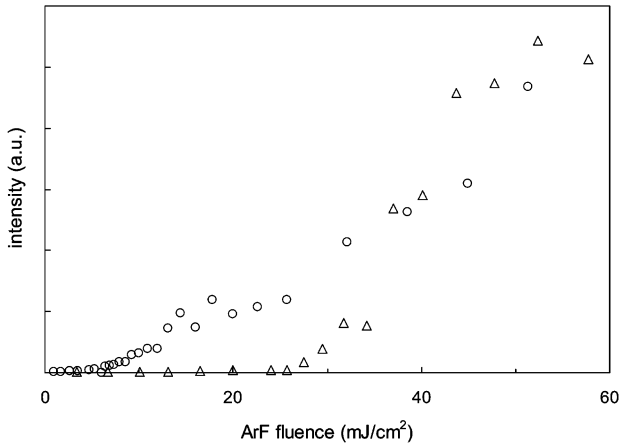

Figure 4. Time-integrated intensities of the prompt emissions at 405.8 (open circles) and 357.3 nm (open triangles) induced by an ArF laser beam off bulk lead targets, as functions of the laser fluence.

very efficient LEAF at a fixed excitation wavelength of 193 nm remained puzzling. This issue was addressed in the next section when time-resolved spectra were analyzed.

Time-Resolved Spectra and Excitation Mechanism. To elucidate the mechanism of the prompt Pb I emissions, time-resolved spectra of various lead lines were taken under four different experimental conditions: (1) two-pulse (1064 + 193 nm) sampling of dissolved lead ion, (2) the same two-pulse sampling of lead carbonate colloids, (3) sampling of the colloids with the ArF laser alone, and (4) sampling of bulk lead with the ArF laser alone. The ICCD gate width was set to 11 ns electronically, which gave an optical gate width of ~2.5 ns. Time slices of the 405.8-nm emissions that are representative of the trend are shown in Figure 5. Three observations could be drawn. First, for cases when only the ArF laser was used (rightmost two panels of Figure 5), marked spectral broadening occurred. For the case of two-pulse sampling of colloids (second panel), spectral broadening was also apparent near the beginning. The widths could not be due to Doppler or Stark broadening, especially for the low laser fluences used here. Given the extremely high plume density near the beginning, the extensive scrambling of the atomic energy levels was probably caused by proximity to other species. Another perturbing agent could be the parent colloidal surface or the bulk lead surface. The absence of broadening in the case of dissolved ion (first panel) was consistent with this latter hypothesis.

Second, for the broadened lines, the evolution of the line width over time was also revealing. For the colloids, the line width gradually shrank from 0.5 nm (fwhm, full width at half-maximum) to the instrumental resolution of 0.2 nm near the end of the ArF laser pulse. This is indicative of the steady depletion of the perturbing agents, such as the volatilization of the colloidal particles and the thinning of the plume. For the case of colloid sampling with the ArF laser alone, the plume was probably heated to ~0.4 eV,[7] and a 200-nm-diameter colloid would vaporize completely in ~10 ns.[17] This is consistent with the experimental results shown in the third panel. For the case of two-pulse sampling shown in the second panel, the colloids were already partially vaporized by the 1064-nm pulse. Line broadening was therefore brief. Of course, for the bulk lead sample shown in the fourth panel, the perturbing agent would last throughout. This could explain the extent and persistence of the broadening for that case. Line reversal, indicative of self-absorption, was also observed for this last case. It would contribute toward the apparent broadening of the spectral line as well.

Third, it was interesting to note that the line broadening for bulk lead (fourth panel) was not as evident initially as the colloid cases, suggesting that the emitting atoms were only weakly perturbed at the early instants. A plausible picture might be as follows: the lead atom thermally desorbed from the bulk was excited to a level ~6.4 eV above the ground state by absorbing a 193-nm photon. At this initial stage, the vapor plume was barely formed and collisional relaxation was ineffective. The lead atom therefore remained highly excited while separating from the bulk. When it finally relaxed to the 4.4-eV upper state of the 405.8-nm transition, the perturbing agents were already far away. It was not until later when the plume turned denser and hotter that rapid relaxation to the 4.4-eV level could occur and broadening of the 405.8-nm line then showed up. For colloids, in contrast, the desorbing lead atoms would see a relatively dense plume early on.

Similar time-resolved spectra of the 357.3-nm emissions are shown in Figure 6. Although the general trends resembled the 405.8-nm emissions shown in Figure 5, two differences concerning the bulk lead case were still noticeable. First, self-absorption was no longer evident. This is expected because the lower state of this transition was 1.3 eV above that of the 405.8-nm transition, and collisional relaxation would be more effective. Second, the 357.3-nm line became narrow near the end. This might be understood this way: As the ArF laser pulse died off, the vapor plume cooled and dispersed rapidly. Relaxation to the 6.13-eV upper level of the 357.3-nm line by collision became less effective, thus increasing the delay between 193-nm photon absorption and 357.3-nm emission. The emitting atom therefore separated further from the perturbing agents. Accordingly, the 357.5-nm line became less broad. In other words, unlike the 4.4-eV level, a hotter and denser plume was required to efficiently relax the highly excited (6.4 eV) Pb atom to the 6.13-eV level. This also explained the higher threshold fluence required for seeing the 357.3-nm line than the 405.8-nm line (Figure 4).

We now postulate that strong perturbation of emitting lead atoms by nearby interacting agents was the hallmark of ArF laser-induced prompt signal. If the interaction could manifestly shift the energy of the 4.4- and the 6.13-eV levels, it might equally shift those levels around 6.4 eV to allow for resonant absorption of 193-nm photons. This should be particularly plausible given the relatively broad (0.49 nm fwhm; see Figure 2) ArF laser line. To

(16) The threshold fluence averaged over the laser spot size was ~5 mJ cm^{-2} in order to start seeing 405.8-nm emissions, as Figure 4 shows. The peak fluence at the spot center would be ~10 mJ cm^{-2}. Using standard laser heating models, one could show that 10 mJ cm^{-2} at 193 nm would heat the lead surface to ~600 K, just enough to melt but not boil the metal; but the vapor pressure was presumably adequate for lead emissions to be detected. In other words, at the threshold fluences, most photons were channeled to heating the target while few were left for inducing fluorescence off lead atoms. Two-photon processes were therefore unlikely. To model laser heating, see for example: Lee, K. C.; Chan, C. S.; Cheung, N. H. *J. Appl. Phys.* **1996**, *79*, 3900−3905.

(17) Reist, P. C. *Aerosol Science and Technology*, 2nd ed.; McGraw-Hill: New York, 1993.

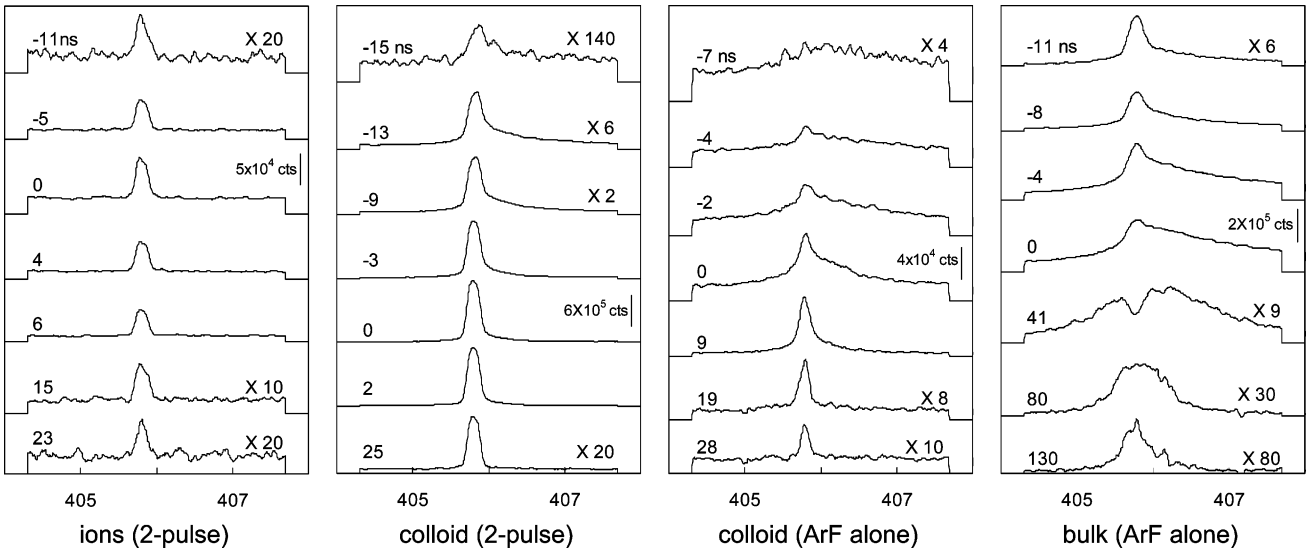

Figure 5. Time-resolved spectra of the 405.8-nm emissions generated under four different experimental conditions: two-pulse analysis of 100 ppm lead ion solution (first panel), two-pulse analysis of lead carbonate colloid suspensions (second panel), analysis of the same colloid suspensions by the ArF laser alone (third panel), and analysis of bulk lead by the ArF laser alone (fourth panel). The [Pb] for the colloid suspensions was 1 ppm. The laser fluences are given in the text, except for the last panel when it was 300 mJ cm^{-2}. Time zero was defined by the peak of the ArF laser pulse. The height of the vertical bar indicates the intensity in CCD counts. Weaker traces were magnified for clarity, with the scale factors shown.

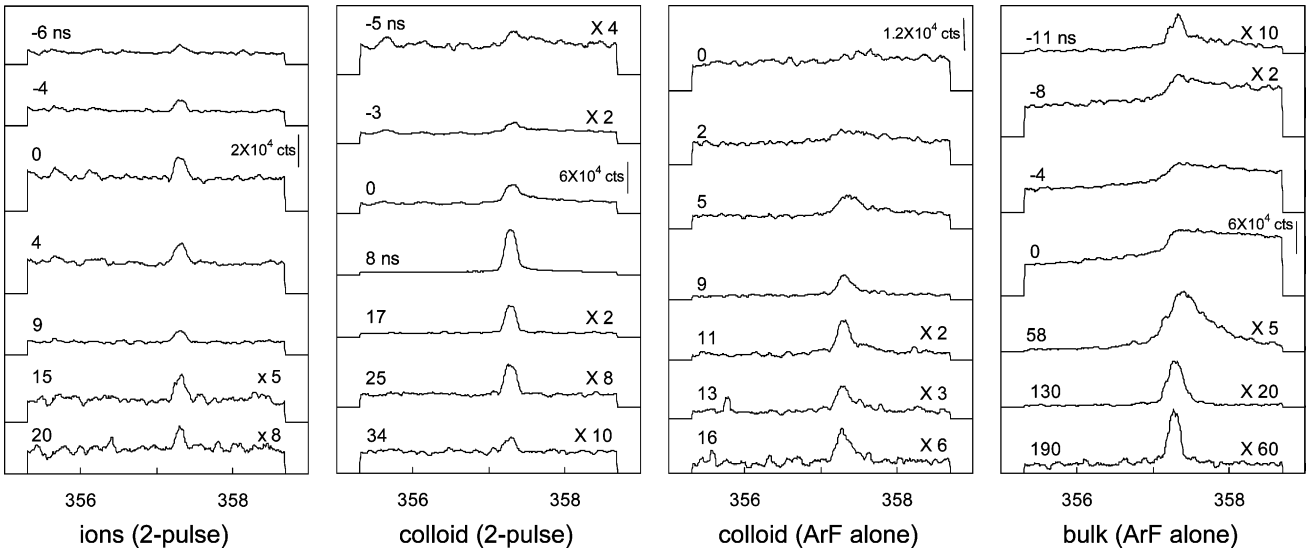

Figure 6. Identical to Figure 5 except the 357.3-nm lead line is shown and 120 ppm [Pb] was used to generate the first panel.

summarize, the entire process might be pictured as follows: The laser pulse ablated the target to form a hot plume. Atoms desorbed from the colloid particles or the bulk by thermal vaporization. The desorbing lead atoms were strongly perturbed by the nearby colloid or bulk surface, or other species in the dense plume. They resonantly absorbed at 193 nm although isolated lead atoms did not. These highly excited lead atoms decayed to lower energy states via collisional relaxation. They further decayed radiatively to produce the various spectral lines. If collisional relaxation was prompt, the emitting atoms would still be perturbed by the nearby agents and the spectral line would be broadened. If relaxation was slow, the emitting atoms would have moved away from the perturbing agents and spectral line broadening became less apparent.

Our findings had analytical implications. It guided us in developing an all-optical technique for sub-ppb analysis of aqueous lead colloids, as we will show in the next section. It also suggested that the technique might be applicable to elements other than lead. After all, most elements and especially metals have dense energy levels around 6.4 eV. Induced resonant absorption at 193 nm might be surprisingly universal.

Signal Optimization and Analytical Performance. As can be seen from Figure 3, the lead emission line at 405.8 nm was the brightest and was therefore adopted as the analytical line. To maximize its signal-to-noise ratio (SNR), two experimental aspects were considered, colloid sample preparation and optical instrumentation.

We explained earlier that colloids as preconcentrated analytes or as perturbing agents would play a key role in the detection of lead. Accordingly, their size could matter. It was mentioned in the Experimental Section that different preparation procedures produced lead carbonate colloids of different sizes. The size

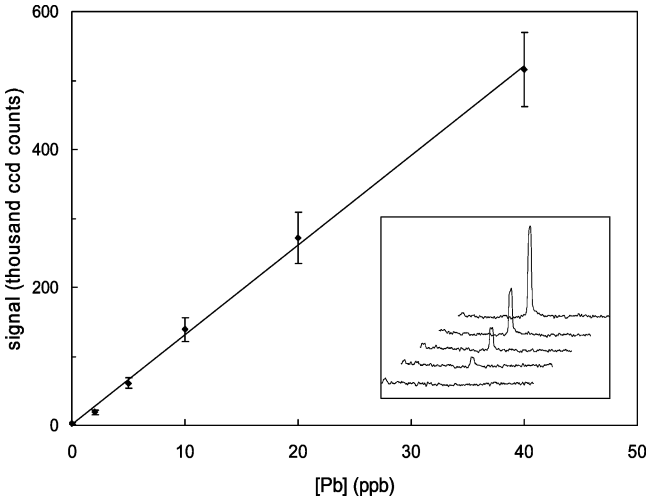

Figure 7. Calibration curve for two-pulse ArF-LEAF analysis of lead carbonate colloids. Ten spectra were taken for each concentration, and the standard deviations are shown as error bars. The best straight line fit is also shown. Inset shows typical spectra corresponding to 0, 5, 10, 20, and 40 ppb [Pb], slightly off-set for clarity.

distributions were monitored by dynamic light scattering. It was found that colloids of ~200 nm in diameter gave the strongest signal. For the same [Pb], larger colloids (880-nm diameter) gave a 2.5× weaker signal.

For the 200-nm colloid sample, filtering through 0.2-μm filters would reduce the signal to less than one-third. This indicated that the 0.2-μm filters would retain most of these colloid particles.

Optical instrumentation affected SNR as well. For the two-pulse approach, four experimental parameters were particularly important. First, the energy and spot size of the 1064-nm beam controlled the amount of colloids sampled and the brightness of the background. Fluences above 23 J cm^{-2} would start to break down pure water. Fluences above 30 J cm^{-2} would generate bright background emissions and would vaporize the colloids prematurely. Too low a fluence would deliver too few colloidal particles to the ArF laser beam. We found that an energy ranging from 15 to 60 mJ/pulse focused to a spot size of ~0.5-mm diameter was suitable. Second, the ArF laser fluence should not exceed 5 J cm^{-2} else luminous plasmas would be produced. The optimal ArF fluence depended on the Nd:YAG laser parameters. For a 1064-nm fluence of ~8 J cm^{-2}, an ArF laser energy of 27 mJ/pulse focused to 3 mm × 0.5 mm was suitable. When a higher Nd:YAG fluence of 30 J cm^{-2} was employed, the ArF laser energy had to be increased to 60 mJ/pulse, presumably because hot water vapor strongly absorbed at 193 nm,[18] and the stronger 1064-nm pulse produced a thicker vapor shield. For these combinations of laser fluences, the 193-nm induced background remained negligible. Nonetheless, the higher fluence (30 J cm^{-2} at 1064 nm and 4 J cm^{-2} at 193 nm) combination gave the maximum sensitivity and was adopted for all subsequent analysis. Third, the ArF laser pulse should be fired after the Nd:YAG laser-induced background had decayed sufficiently and before the trailing colloids had dispersed. We found that a delay of 2.5 μs was suitable for the optimized range of laser energy. Fourth, the ICCD was gated on 30 ns before the ArF laser was fired and remained on for 100 ns to fully capture the analyte signal while rejecting unwanted noise. Other experimental parameters, such as the slit width of the spectrometer and the number of events to be averaged, were found to be less critical. A slit width of 220 μm was adopted, and 300 events were accumulated for each analytical spectrum.

When the experimental conditions were optimized, even trace amounts of lead carbonate colloids became detectable. To quantify the results, we defined the gross signal as the average intensity (ICCD counts) in the spectral region from 405.75 through 405.85 nm, bracketing the Pb 405.8-nm line. Background was defined as the average intensity in two neighboring regions from 405.20 through 405.39 nm and 406.26 through 406.45 nm. The net signal was defined as the gross signal minus the background. Figure 7 plots the net signal against Pb concentration. The [Pb] of the standard samples were confirmed using ICPMS, and the deviations were all within 10%. At each concentration (blank, 2, 5, 10, 20, and 40 ppb), 10 data points were taken, and every data point was an accumulation of 300 events. The best straight line was also drawn. The correlation R^2 was 0.9985. The slope m was 1.3 × 10^4 counts ppb^{-1}. Typical spectra are shown in the inset of Figure 7. The standard deviation σ of the blank signal was 1.0 × 10^3 counts. The detection limit ($3\sigma/m$) was therefore estimated to be 0.24 ppb. Similar experiments were performed on aqueous colloids of PbO. Preliminary results indicated detection sensitivity comparable to that of the carbonates.

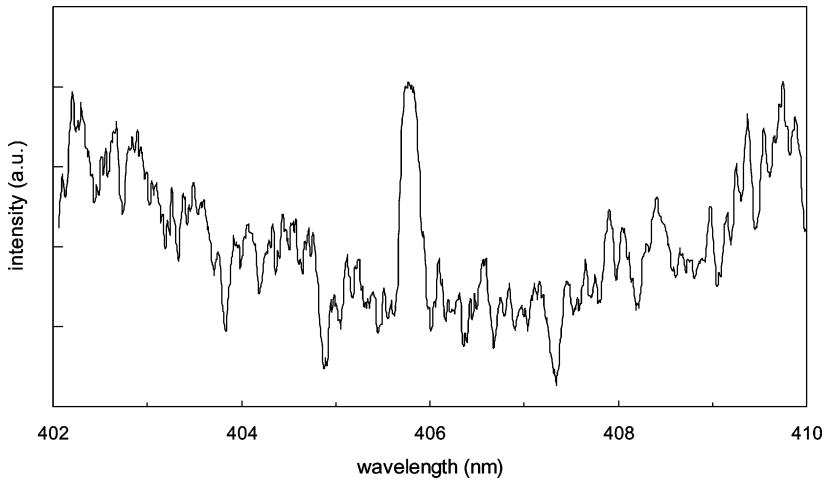

Figure 8. Spectrum produced by two-pulse ArF-LEAF analysis of household tap water, showing the 405.8-nm lead emission line.

We applied the two-pulse technique to the analysis of tap water collected from faucets in our laboratory. If there should be lead colloids, they were likely to be either carbonates or oxides of submicrometer size. Larger colloids would readily sediment. Figure 8 shows a typical spectrum of the tap water analyzed. While lead emissions at 405.8 nm were clearly observed, the background was also noticeably stronger than that of the standard samples. As a result, the calibration curve shown in Figure 7 could not be used to quantify the amount of lead. Instead, the standard addition method was used and the amount of lead was estimated to be $\sim 2.1 \pm 0.3$ ppb. This should be indicative of the amount of lead present in the form of submicrometer-size colloids. To cross-check our results, aliquots of the same tap water sample, some filtered with 0.2-μm filters, were digested and analyzed by ICPMS for total lead. The results were 1.4 ± 0.5 and 2.1 ± 0.15 ppb for the samples with and without filtering, respectively. Given the uncertainty in the size and the chemical composition of the sample colloids, the difference in the two analytical results was to be expected.

The ArF-LEAF technique was also applied to submicrometer colloids of iron oxide and gold and to bulk alloys of copper and aluminum. Prompt emissions from atomic iron, gold, copper, aluminum, and other minor components in the metal alloys were all observed. More systematic analyses of these other systems were underway.

CONCLUSION

We demonstrated an all-optical technique for real-time and on-line analysis of trace amounts of submicrometer-size lead carbonate colloids suspended in water. A Nd:YAG laser pulse at 1064 nm and 30 J cm^{-2} ablated the sample solution to create an expanding plume. The colloid particles, being heavier, trailed behind and became concentrated. They were then intercepted by an ArF laser pulse at 193 nm and 4 J cm^{-2} that further vaporized the colloids and induced atomic fluorescence from the desorbing lead atoms. Very sensitive detection of lead was possible. The detection limit was shown to be $\sim$0.24 ppb for colloids of 200 nm in diameter. For larger colloids, the signal would decrease.

Other than lead carbonate, the technique was found to be applicable to practically all systems tested so far. They included colloids of lead and iron oxides as well as gold and bulk alloys of lead, copper, and aluminum. Tap water was also analyzed, and lead emissions were clearly observable.

The apparatus was identical to a conventional LIPS setup, sharing most of the LIPS advantages but orders of magnitude more sensitive. It will be a valuable technique for elemental analysis of particulates and bulk targets at stand-off distances.

ACKNOWLEDGMENT

We thank G. Hu and S.Y. Liu for the dynamic light scattering measurements, and K.H. Wong of Hong Kong Polytechnic University for making available their ball grinder facility. This work is supported by the Faculty Research Grant of the Hong Kong Baptist University and the Earmarked Research Grant of the Research Grants Council of Hong Kong under Grant HKBU 2106/01P.

Received for review August 19, 2004. Accepted October 15, 2004.

AC048764A

(18) Kessler, W. J.; Carleton, K. L.; Marinelli, W. J. *J. Quant. Spectrosc. Radiat. Transfer* **1993**, *50*, 39−46.